# 1

# What Does "Control of Robots" Involve?

The present textbook focuses on the interaction between robotics and electrical engineering and more specifically, in the area of *automatic control*. From this interaction emerges what we call *robot control*.

Loosely speaking (in this textbook), robot control consists in studying how to make a robot manipulator perform a task and in materializing the results of this study in a lab prototype.

In spite of the numerous existing commercial robots, robot control design is still a field of intensive study among robot constructors and research centers. Some specialists in automatic control might argue that today's industrial robots are already able to perform a variety of complex tasks and therefore, at first sight, the research on robot control is not justified anymore. Nevertheless, not only is research on robot control an interesting topic by itself but it also offers important theoretical challenges and more significantly, its study is indispensable in specific tasks which cannot be performed by the present commercial robots.

As a general rule, control design may be divided roughly into the following steps:

- familiarization with the physical system under consideration;
- modeling;
- control specifications.

In the sequel we develop further on these stages, emphasizing specifically their application in robot control.

## 1.1 Familiarization with the Physical System under Consideration

On a general basis, during this stage one must determine the physical variables of the system whose behavior is desired to control. These may be temperature, pressure, displacement, velocity, *etc.* These variables are commonly referred to as the system's *outputs*. In addition to this, we must also clearly identify those variables that are available and that have an influence on the behavior of the system and more particularly, on its outputs. These variables are referred to as *inputs* and may correspond for instance, to the opening of a valve, voltage, torque, force, *etc.*

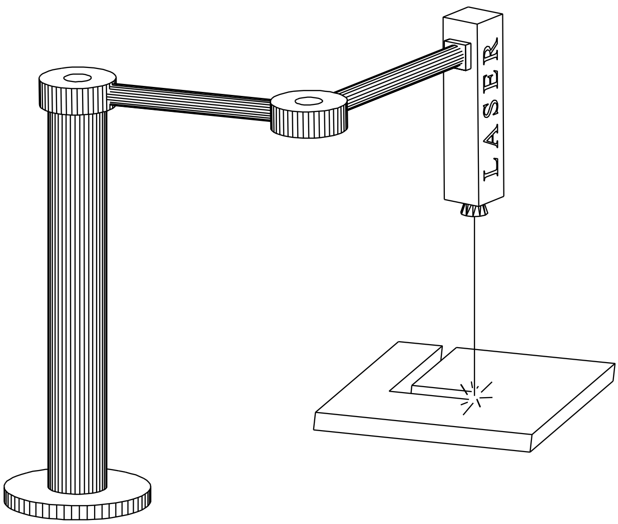


**Figure 1.1.** Freely moving robot

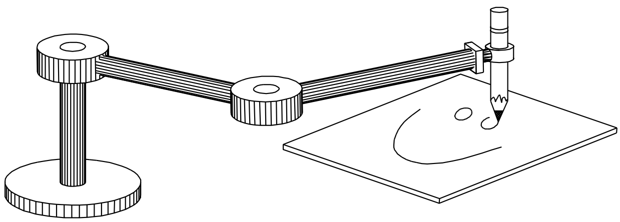

**Figure 1.2.** Robot interacting with its environment

In the particular case of robot manipulators, there is a wide variety of outputs – temporarily denoted by $\boldsymbol{y}$ – whose behavior one may wish to control.

For robots moving freely in their *workspace*, *i.e.* without interacting with their environment (*cf.* Figure 1.1) as for instance robots used for painting, "pick and place", laser cutting, *etc.*, the output $\boldsymbol{y}$ to be controlled, may correspond to the joint positions $\boldsymbol{q}$ and joint velocities $\dot{\boldsymbol{q}}$ or alternatively, to the position and orientation of the end-effector (also called end-tool).

For robots such as the one depicted in Figure 1.2 that have physical contact with their environment, *e.g.* to perform tasks involving polishing, deburring of materials, high quality assembling, *etc.*, the output $\boldsymbol{y}$ may include the torques and forces $\boldsymbol{f}$ exerted by the end-tool over its environment.

Figure 1.3 shows a manipulator holding a marked tray, and a camera which provides an image of the tray with marks. The output $\boldsymbol{y}$ in this system may correspond to the coordinates associated to each of the marks with reference to a screen on a monitor. Figure 1.4 depicts a manipulator whose end-effector has a camera attached to capture the scenery of its environment. In this case, the output $\boldsymbol{y}$ may correspond to the coordinates of the dots representing the marks on the screen and which represent visible objects from the environment of the robot.

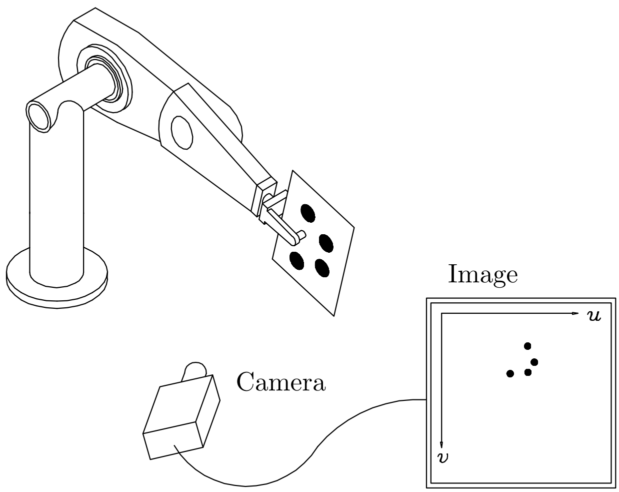


**Figure 1.3.** Robotic system: fixed camera

From these examples we conclude that the corresponding output $\boldsymbol{y}$ of a robot system – involved in a specific class of tasks – may in general, be of the form

$$\boldsymbol{y} = \boldsymbol{y}(\boldsymbol{q}, \dot{\boldsymbol{q}}, \boldsymbol{f}) .$$

On the other hand, the input variables, that is, those that may be modified to affect the evolution of the output, are basically the torques and forces $\boldsymbol{\tau}$ applied by the actuators over the robot's joints. In Figure 1.5 we show

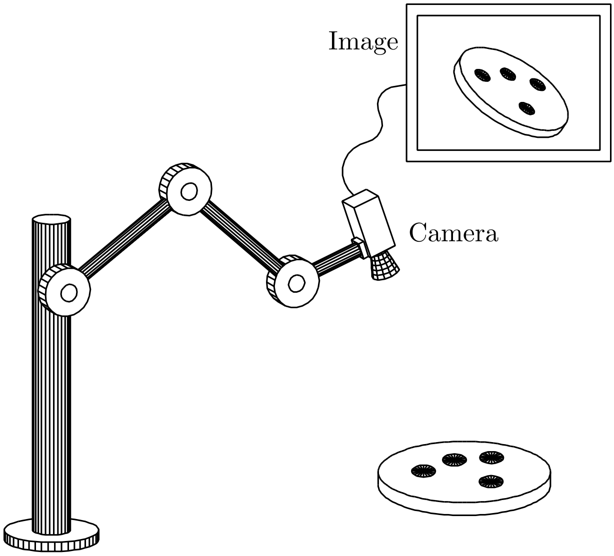


**Figure 1.4.** Robotic system: camera in hand

the block-diagram corresponding to the case when the outputs are the joint positions and velocities, that is,

$$\boldsymbol{y} = \boldsymbol{y}(\boldsymbol{q}, \dot{\boldsymbol{q}}, \boldsymbol{f}) = \begin{bmatrix} \boldsymbol{q} \\ \dot{\boldsymbol{q}} \end{bmatrix}$$

while $\boldsymbol{\tau}$ is the input. In this case notice that for robots with $n$ joints one has, in general, $2n$ outputs and $n$ inputs.

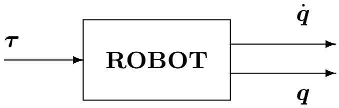


**Figure 1.5.** Input–output representation of a robot

## 1.2 Dynamic Model

At this stage, one determines the mathematical model which relates the input variables to the output variables. In general, such mathematical representation of the system is realized by ordinary differential equations. The system's mathematical model is obtained typically via one of the two following techniques.

- *Analytical*: this procedure is based on physical laws of the system's motion. This methodology has the advantage of yielding a mathematical model as precise as is wanted.
- *Experimental*: this procedure requires a certain amount of experimental data collected from the system itself. Typically one examines the system's behavior under specific input signals. The model so obtained is in general more imprecise than the analytic model since it largely depends on the inputs and the operating point[1]. However, in many cases it has the advantage of being much easier and quicker to obtain.

On certain occasions, at this stage one proceeds to a simplification of the system model to be controlled in order to design a relatively simple controller. Nevertheless, depending on the degree of simplification, this may yield malfunctioning of the overall controlled system due to potentially neglected physical phenomena. The ability of a control system to cope with errors due to neglected dynamics is commonly referred to as *robustness*. Thus, one typically is interested in designing robust controllers.

In other situations, after the modeling stage one performs the *parametric identification*. The objective of this task is to obtain the numerical values of different physical parameters or quantities involved in the dynamic model. The identification may be performed via techniques that require the measurement of inputs and outputs to the controlled system.

The dynamic model of robot manipulators is typically derived in the analytic form, that is, using the laws of physics. Due to the mechanical nature of robot manipulators, the laws of physics involved are basically the laws of mechanics.

On the other hand, from a dynamical systems viewpoint, an $n$-DOF system may be considered as a *multivariable nonlinear* system. The term "multivariable" denotes the fact that the system has multiple (*e.g.* $n$) inputs (the forces and torques $\boldsymbol{\tau}$ applied to the joints by the electromechanical, hydraulic or pneumatic actuators) and, multiple ($2n$) state variables typically associated to the $n$ positions $\boldsymbol{q}$, and $n$ joint velocities $\dot{\boldsymbol{q}}$. In Figure 1.5 we depict the corresponding block-diagram assuming that the state variables also correspond to the outputs. The topic of robot dynamics is presented in Chapter 3. In Chapter 5 we provide the specific dynamic model of a two-DOF prototype of a robot manipulator that we use to illustrate through examples, the performance of the controllers studied in the succeeding chapters. Readers interested in the aspects of dynamics are invited to see the references listed on page 16.

As was mentioned earlier, the dynamic models of robot manipulators are in general characterized by ordinary nonlinear and nonautonomous[2] differential equations. This fact limits considerably the use of control techniques

[1] That is the working regime.

[2] That is, they depend on the state variables and time. See Chapter 2.

tailored for linear systems, in robot control. In view of this and the present requirements of precision and rapidity of robot motion it has become necessary to use increasingly sophisticated control techniques. This class of control systems may include nonlinear and adaptive controllers.

## 1.3 Control Specifications

During this last stage one proceeds to dictate the desired characteristics for the control system through the definition of control objectives such as:

- stability;
- regulation (position control);
- trajectory tracking (motion control);
- optimization.

The most important property in a control system, in general, is *stability*. This fundamental concept from control theory basically consists in the property of a system to go on working at a regime or *closely* to it *for ever*.

Two techniques of analysis are typically used in the analytical study of the stability of controlled robots. The first is based on the so-called *Lyapunov* stability theory. The second is the so-called *input–output* stability theory. Both techniques are complementary in the sense that the interest in Lyapunov theory is the study of stability of the system using a *state* variables description, while in the second one, we are interested in the stability of the system from an input–output perspective. In this text we concentrate our attention on Lyapunov stability in the development and analysis of controllers. The foundations of Lyapunov theory are presented in the Chapter 2.

In accordance with the adopted definition of a robot manipulator's output $\boldsymbol{y}$, the control objectives related to *regulation* and *trajectory tracking* receive special names. In particular, in the case when the output $\boldsymbol{y}$ corresponds to the joint position $\boldsymbol{q}$ and velocity $\dot{\boldsymbol{q}}$, we refer to the control objectives as "*position* control in joint coordinates" and "*motion* control in joint coordinates" respectively. Or we may simply say "position" and "motion" control respectively. The relevance of these problems motivates a more detailed discussion which is presented next.

## 1.4 Motion Control of Robot Manipulators

The simplest way to specify the movement of a manipulator is the so-called "point-to-point" method. This methodology consists in determining a series of points in the manipulator's workspace, which the end-effector is required to pass through (*cf.* Figure 1.6). Thus, the position control problem consists in making the end-effector go to a specified point regardless of the trajectory followed from its initial configuration.

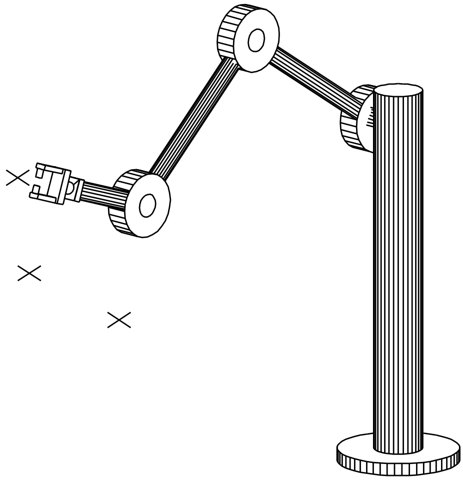

**Figure 1.6.** Point-to-point motion specification

A more general way to specify a robot's motion is via the so-called (continuous) trajectory. In this case, a (continuous) curve, or path in the state space and parameterized in time, is available to achieve a desired task. Then, the *motion* control problem consists in making the end-effector follow this trajectory as closely as possible (*cf.* Figure 1.7). This control problem, whose study is our central objective, is also referred to as trajectory tracking control.

Let us briefly recapitulate a simple formulation of robot control which, as a matter of fact, is a particular case of motion control; that is, the position control problem. In this formulation the specified trajectory is simply a point in the workspace (which may be translated under appropriate conditions into a point in the joint space). The position control problem consists in driving the manipulator's end-effector (resp. the joint variables) to the desired position, regardless of the initial posture.

The topic of motion control may in its turn, be fitted in the more general framework of the so-called *robot navigation*. The robot navigation problem consists in solving, in one single step, the following subproblems:

- path planning;
- trajectory generation;
- control design.

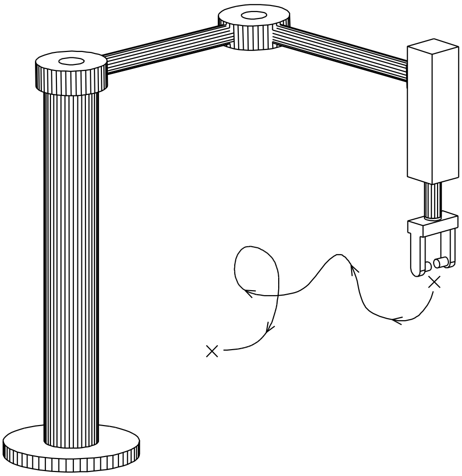

**Figure 1.7.** Trajectory motion specification

*Path planning* consists in determining a curve in the state space, connecting the initial and final desired posture of the end-effector, while avoiding any obstacle. Trajectory generation consists in parameterizing in time the so-obtained curve during the path planning. The resulting time-parameterized trajectory which is commonly called the *reference* trajectory, is obtained primarily in terms of the coordinates in the workspace. Then, following the so-called method of *inverse kinematics* one may obtain a time-parameterized trajectory for the joint coordinates. The control design consists in solving the control problem mentioned above.

The main interest of this textbook is the study of motion controllers and more particularly, the analysis of their inherent stability in the sense of Lyapunov. Therefore, we assume that the problems of path planning and trajectory generation are previously solved.

The dynamic models of robot manipulators possess parameters which depend on physical quantities such as the mass of the objects possibly held by the end-effector. This mass is typically unknown, which means that the values of these parameters are unknown. The problem of controlling systems with unknown parameters is the main objective of the *adaptive* controllers. These owe their name to the addition of an adaptation law which updates on-line, an estimate of the unknown parameters to be used in the control law. This motivates the study of adaptive control techniques applied to robot control. In the past two decades a large body of literature has been devoted to the adaptive control of manipulators. This problem is examined in Chapters 15 and 16.

We must mention that in view of the scope and audience of the present textbook, we have excluded some control techniques whose use in robot motion control is supported by a large number of publications contributing both theoretical and experimental achievements. Among such strategies we mention the so-called passivity-based control, variable-structure control, learning control, fuzzy control and neural-networks-based. These topics, which demand a deeper knowledge of control and stability theory, may make part of a second course on robot control.

## Bibliography

A number of concepts and data related to robot manipulators may be found in the introductory chapters of the following textbooks.


- Paul R., 1981, *"Robot manipulators: Mathematics programming and control"*, MIT Press, Cambridge, MA.
- Asada H., Slotine J. J., 1986, *"Robot analysis and control "*, Wiley, New York.
- Fu K., Gonzalez R., Lee C., 1987, *"Robotics: Control, sensing, vision and intelligence"*, McGraw–Hill.
- Craig J., 1989, *"Introduction to robotics: Mechanics and control"*, Addison-Wesley, Reading, MA.
- Spong M., Vidyasagar M., 1989, *"Robot dynamics and control"*, Wiley, New York.
- Yoshikawa T., 1990, *"Foundations of robotics: Analysis and control"*, The MIT Press.
- Nakamura Y., 1991, *"Advanced robotics: Redundancy and optimization"*, Addison–Wesley, Reading, MA.
- Spong M., Lewis F. L., Abdallah C. T., 1993, *"Robot control: Dynamics, motion planning and analysis"*, IEEE Press, New York.
- Lewis F. L., Abdallah C. T., Dawson D. M., 1993, *"Control of robot manipulators"*, Macmillan Pub. Co.
- Murray R. M., Li Z., Sastry S., 1994, *"A mathematical introduction to robotic manipulation"*, CRC Press, Inc., Boca Raton, FL.
- Qu Z., Dawson D. M., 1996, *"Robust tracking control of robot manipulators"*, IEEE Press, New York.
- Canudas C., Siciliano B., Bastin G., (Eds), 1996, *"Theory of robot control"*, Springer-Verlag, London.
- Arimoto S., 1996, *"Control theory of non–linear mechanical systems"*, Oxford University Press, New York.
- Sciavicco L., Siciliano B., 2000, *"Modeling and control of robot manipulators"*, Second Edition, Springer-Verlag, London.

- de Queiroz M., Dawson D. M., Nagarkatti S. P., Zhang F., 2000, *"Lyapunov–based control of mechanical systems"*, Birkhäuser, Boston, MA.

Robot dynamics is thoroughly discussed in Spong, Vidyasagar (1989) and Sciavicco, Siciliano (2000).

To read more on the topics of force control, impedance control and hybrid motion/force see among others, the texts of Asada, Slotine (1986), Craig (1989), Spong, Vidyasagar (1989), and Sciavicco, Siciliano (2000), previously cited, and the book

- Natale C., 2003, *"Interaction control of robot manipulators"*, Springer, Germany.
- Siciliano B., Villani L., *"Robot force control"*, 1999, Kluwer Academic Publishers, Norwell, MA.

Aspects of stability in the input–output framework (in particular, passivity-based control) are studied in the first part of the book

- Ortega R., Loría A., Nicklasson P. J. and Sira-Ramírez H., 1998, *"Passivity-based control of Euler-Lagrange Systems Mechanical, Electrical and Electromechanical Applications"*, Springer-Verlag: London, Communications and Control Engg. Series.

In addition, we may mention the following classic texts.

- Raibert M., Craig J., 1981, *"Hybrid position/force control of manipulators"*, ASME Journal of Dynamic Systems, Measurement and Control, June.
- Hogan N., 1985, *"Impedance control: An approach to manipulation. Parts I, II, and III"*, ASME Journal of Dynamic Systems, Measurement and Control, Vol. 107, March.
- Whitney D., 1987, *" Historical perspective and state of the art in robot force control"*, The International Journal of Robotics Research, Vol. 6, No. 1, Spring.

The topic of robot navigation may be studied from

- Rimon E., Koditschek D. E., 1992, *"Exact robot navigation using artificial potential functions"*, IEEE Transactions on Robotics and Automation, Vol. 8, No. 5, October.

Several theoretical and technological aspects on the guidance of manipulators involving the use of vision sensors may be consulted in the following books.

- Hashimoto K., 1993, *"Visual servoing: Real–time control of robot manipulators based on visual sensory feedback"*, World Scientific Publishing Co., Singapore.
- Corke P.I., 1996, *"Visual control of robots: High–performance visual servoing"*, Research Studies Press Ltd., Great Britain.
- Vincze M., Hager G. D., 2000, *"Robust vision for vision-based control of motion"*, IEEE Press, Washington, USA.


The definition of robot manipulator is taken from


- United Nations/Economic Commission for Europe and International Federation of Robotics, 2001, *"World robotics 2001"*, United Nation Publication *sales No.* GV.E.01.0.16, ISBN 92–1–101043–8, ISSN 1020–1076, Printed at United Nations, Geneva, Switzerland.


We list next some of the most significant journals focused on robotics research.

- *Advanced Robotics*,
- *Autonomous Robots*,
- *IASTED International Journal of Robotics and Automation*
- *IEEE/ASME Transactions on Mechatronics*,
- *IEEE Transactions on Robotics and Automation*[3],
- *IEEE Transactions on Robotics*,
- *Journal of Intelligent and Robotic Systems*,
- *Journal of Robotic Systems*,
- *Mechatronics*,
- *The International Journal of Robotics Research*,
- *Robotica.*

Other journals, which in particular, provide a discussion forum on robot control are

- *ASME Journal of Dynamic Systems, Measurement and Control*,
- *Automatica*,
- *IEEE Transactions on Automatic Control*,
- *IEEE Transactions on Industrial Electronics*,
- *IEEE Transactions on Systems, Man, and Cybernetics*,
- *International Journal of Adaptive Control and Signal Processing*,
- *International Journal of Control*,
- *Systems and Control Letters.*

[3] Until June 2004 only.

# 5

# Case Study: The Pelican Prototype Robot

The purpose of this chapter is twofold: first, to present in detail the model of the experimental robot arm of the Robotics lab. from the CICESE Research Center, Mexico. Second, to review the topics studied in the previous chapters and to discuss, through this case study, the topics of direct kinematics and inverse kinematics, which are fundamental in determining robot models.

For the Pelican, we derive the full dynamic model of the prototype; in particular, we present the numerical values of all the parameters such as mass, inertias, lengths to centers of mass, *etc.* This is used throughout the rest of the book in numerous examples to illustrate the performance of the controllers that we study. We emphasize that *all* of these examples contain *experimentation* results.

Thus, the chapter is organized in the following sections:

- direct kinematics;
- inverse kinematics;
- dynamic model;
- properties of the dynamic model;
- reference trajectories.

For analytical purposes, further on, we refer to Figure 5.2, which represents the prototype schematically. As is obvious from this figure, the prototype is a planar arm with two links connected through revolute joints, *i.e.* it possesses 2 DOF. The links are driven by two electrical motors located at the "shoulder" (base) and at the "elbow". This is a direct-drive mechanism, *i.e.* the axes of the motors are connected directly to the links without gears or belts.

The manipulator arm consists of two rigid links of lengths $l_1$ and $l_2$, masses $m_1$ and $m_2$ respectively. The robot moves about on the plane $x$–$y$ as is illustrated in Figure 5.2. The distances from the rotating axes to the centers of mass are denoted by $l_{c1}$ and $l_{c2}$ for links 1 and 2, respectively. Finally, $I_1$ and

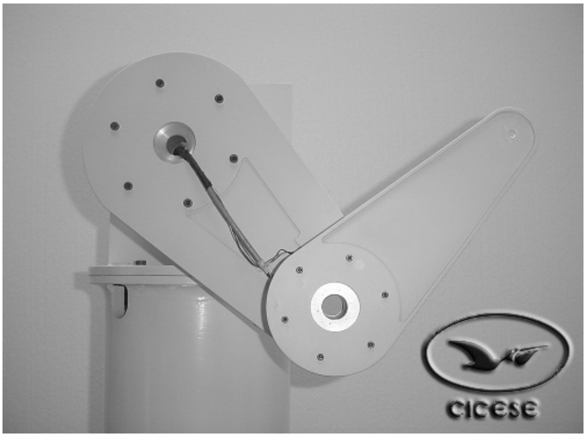


**Figure 5.1.** Pelican: experimental robot arm at CICESE, Robotics lab.

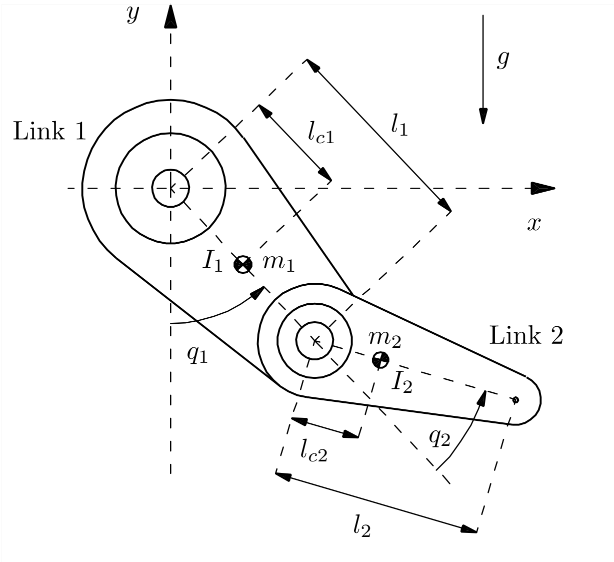


**Figure 5.2.** Diagram of the 2-DOF Pelican prototype robot

$I_2$ denote the moments of inertia of the links with respect to the axes that pass through the respective centers of mass and are parallel to the axis $x$. The degrees of freedom are associated with the angle $q_1$, which is measured from the vertical position, and $q_2$, which is measured relative to the extension of the first link toward the second link, both being positive counterclockwise. The vector of joint positions $\boldsymbol{q}$ is defined as

$$\boldsymbol{q} = [q_1 \quad q_2]^T .$$

The meaning of the diverse constant parameters involved as well as their numerical values are summarized in Table 5.1.

**Table 5.1.** Physical parameters of Pelican robot arm

| **Description** | **Notation** | **Value** | **Units** |
|---|---|---|---|
| Length of Link 1 | $l_1$ | 0.26 | m |
| Length of Link 2 | $l_2$ | 0.26 | m |
| Distance to the center of mass (Link 1) | $l_{c1}$ | 0.0983 | m |
| Distance to the center of mass (Link 2) | $l_{c2}$ | 0.0229 | m |
| Mass of Link 1 | $m_1$ | 6.5225 | kg |
| Mass of Link 2 | $m_2$ | 2.0458 | kg |
| Inertia rel. to center of mass (Link 1) | $I_1$ | 0.1213 | kg $\mathrm{m}^2$ |
| Inertia rel. to center of mass (Link 2) | $I_2$ | 0.0116 | kg $\mathrm{m}^2$ |
| Gravity acceleration | $g$ | 9.81 | $\mathrm{m/s}^2$ |

## 5.1 Direct Kinematics

The problem of direct kinematics for robot manipulators is formulated as follows. Consider a robot manipulator of $n$ degrees-of-freedom placed on a fixed surface. Define a reference frame also fixed at some point on this surface. This reference frame is commonly referred to as 'base reference frame'. The problem of deriving the direct kinematic model of the robot consists in expressing the position and orientation (when the latter makes sense) of a reference frame fixed to the end of the last link of the robot, referred to the base reference frame in terms of the joint coordinates of the robot. The solution to the so-formulated problem from a mathematical viewpoint, reduces to solving a geometrical problem which always has a closed-form solution.

Regarding the Pelican robot, we start by defining the reference frame of base as a Cartesian coordinated system in two dimensions with its origin located exactly on the first joint of the robot, as is illustrated in Figure 5.2. The Cartesian coordinates $x$ and $y$ determine the position of the tip of the second link with respect to the base reference frame. Notice that for the present case study of a 2-DOF system, the orientation of the end-effector of the arm makes no sense. One can clearly appreciate that both Cartesian coordinates, $x$ and

$y$, depend on the joint coordinates $q_1$ and $q_2$. Precisely it is this correlation that defines the direct kinematic model,

$$\begin{bmatrix} x \\ y \end{bmatrix} = \boldsymbol{\varphi}(q_1, q_2)\,,$$

where $\boldsymbol{\varphi} : \mathbb{R}^2 \rightarrow \mathbb{R}^2$.

For the case of this robot with 2 DOF, it is immediate to verify that the direct kinematic model is given by

$$\begin{aligned} x &= l_1 \sin(q_1) + l_2 \sin(q_1 + q_2) \\ y &= -l_1 \cos(q_1) - l_2 \cos(q_1 + q_2)\,. \end{aligned}$$

From this model is obtained: the following relation between the velocities

$$\begin{aligned} \begin{bmatrix} \dot{x} \\ \dot{y} \end{bmatrix} &= \begin{bmatrix} l_1 \cos(q_1) + l_2 \cos(q_1 + q_2) & l_2 \cos(q_1 + q_2) \\ l_1 \sin(q_1) + l_2 \sin(q_1 + q_2) & l_2 \sin(q_1 + q_2) \end{bmatrix} \begin{bmatrix} \dot{q}_1 \\ \dot{q}_2 \end{bmatrix} \\ &= J(\boldsymbol{q}) \begin{bmatrix} \dot{q}_1 \\ \dot{q}_2 \end{bmatrix} \end{aligned}$$

where $J(\boldsymbol{q}) = \dfrac{\partial \boldsymbol{\varphi}(\boldsymbol{q})}{\partial \boldsymbol{q}} \in \mathbb{R}^{2\times 2}$ is called the analytical Jacobian matrix or simply, the Jacobian of the robot. Clearly, the following relationship between accelerations also holds,

$$\begin{bmatrix} \ddot{x} \\ \ddot{y} \end{bmatrix} = \left[ \frac{d}{dt} J(\boldsymbol{q}) \right] \begin{bmatrix} \dot{q}_1 \\ \dot{q}_2 \end{bmatrix} + J(\boldsymbol{q}) \begin{bmatrix} \ddot{q}_1 \\ \ddot{q}_2 \end{bmatrix}.$$

The procedure by which one computes the derivatives of the Jacobian and thereby obtains expressions for the velocities in Cartesian coordinates, is called differential kinematics. This topic is not studied in more detail in this textbook since *we* do not use it for control.

## 5.2 Inverse Kinematics

The inverse kinematic model of robot manipulators is of great importance from a practical viewpoint. This model allows us to obtain the joint positions $\boldsymbol{q}$ in terms of the position and orientation of the end-effector of the last link referred to the base reference frame. For the case of the Pelican prototype robot, the inverse kinematic model has the form

$$\begin{bmatrix} q_1 \\ q_2 \end{bmatrix} = \boldsymbol{\varphi}^{-1}(x, y)$$

where $\boldsymbol{\varphi}^{-1} : \Theta \to \mathbb{R}^2$ and $\Theta \subseteq \mathbb{R}^2$.

The derivation of the inverse kinematic model is in general rather complex and, in contrast to the direct kinematics problem, it may have multiple solutions or no solution at all! The first case is illustrated in Figure 5.3. Notice that for the same position (in Cartesian coordinates $x$, $y$) of the arm tip there exist two possible configurations of the links, *i.e.* two possible values for $\boldsymbol{q}$.

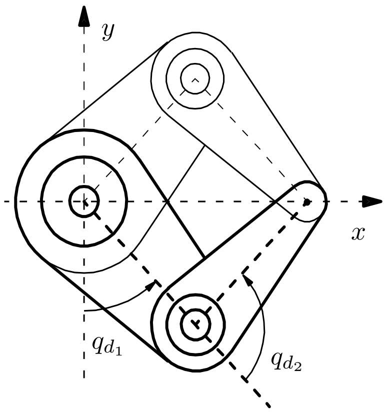


**Figure 5.3.** Two solutions to the inverse kinematics problem

So we see that even for this relatively simple robot configuration there exist more than one solution to the inverse kinematics problem.

The practical interest of the inverse kinematic model relies on its utility to define desired joint positions $\boldsymbol{q}_d = [q_{d_1} \;\; q_{d_2}]^T$ from specified desired positions $x_d$ and $y_d$ for the robot's end-effector. Indeed, note that physically, it is more intuitive to specify a task for a robot in end-effector coordinates so that interest in the inverse kinematics problem increases with the complexity of the manipulator (number of degrees of freedom).

Thus, let us now make our this discussion more precise by analytically computing the solutions $\begin{bmatrix} q_{d_1} \\ q_{d_2} \end{bmatrix} = \boldsymbol{\varphi}^{-1}(x_d, y_d)$. The desired joint positions $\boldsymbol{q}_d$ can be computed using tedious but simple trigonometric manipulations to obtain

$$q_{d_1} = \tan^{-1}\left(\frac{x_d}{-y_d}\right) - \tan^{-1}\left(\frac{l_2 \sin(q_{d_2})}{l_1 + l_2 \cos(q_{d_2})}\right)$$

$$q_{d_2} = \cos^{-1}\left(\frac{x_d^2 + y_d^2 - l_1^2 - l_2^2}{2 l_1 l_2}\right) .$$

The desired joint velocities and accelerations may be obtained via the *differential* kinematics[1] and its time derivative. In doing this one must keep in mind that the expressions obtained are valid only as long as the robot does not "fall" into a singular configuration, that is, as long as the Jacobian $J(\boldsymbol{q}_d)$ is square and nonsingular. These expressions are

$$\begin{bmatrix} \dot{q}_{d_1} \\ \dot{q}_{d_2} \end{bmatrix} = J^{-1}(\boldsymbol{q}_d) \begin{bmatrix} \dot{x}_d \\ \dot{y}_d \end{bmatrix}$$

$$\begin{bmatrix} \ddot{q}_{d_1} \\ \ddot{q}_{d_2} \end{bmatrix} = \underbrace{-J^{-1}(\boldsymbol{q}_d) \left[\frac{d}{dt} J(\boldsymbol{q}_d)\right] J^{-1}(\boldsymbol{q}_d)}_{\frac{d}{dt}\left[J^{-1}(\boldsymbol{q}_d)\right]} \begin{bmatrix} \dot{x}_d \\ \dot{y}_d \end{bmatrix} + J^{-1}(\boldsymbol{q}_d) \begin{bmatrix} \ddot{x}_d \\ \ddot{y}_d \end{bmatrix}$$

where $J^{-1}(\boldsymbol{q}_d)$ and $\frac{d}{dt}\left[J(\boldsymbol{q}_d)\right]$ denote the inverse of the Jacobian matrix and its time derivative respectively, evaluated at $\boldsymbol{q} = \boldsymbol{q}_d$. These are given by

$$J^{-1}(\boldsymbol{q}_d) = \begin{bmatrix} \dfrac{\mathrm{S}_{12}}{l_1 \mathrm{S}_2} & -\dfrac{\mathrm{C}_{12}}{l_1 \mathrm{S}_2} \\ \dfrac{-l_1 \mathrm{S}_1 - l_2 \mathrm{S}_{12}}{l_1 l_2 \mathrm{S}_2} & \dfrac{l_1 \mathrm{C}_1 + l_2 \mathrm{C}_{12}}{l_1 l_2 \mathrm{S}_2} \end{bmatrix},$$

and

$$\frac{d}{dt}\left[J(\boldsymbol{q}_d)\right] = \begin{bmatrix} -l_1 \mathrm{S}_1 \dot{q}_{d_1} - l_2 \mathrm{S}_{12}(\dot{q}_{d_1} + \dot{q}_{d_2}) & -l_2 \mathrm{S}_{12}(\dot{q}_{d_1} + \dot{q}_{d_2}) \\ l_1 \mathrm{C}_1 \dot{q}_{d_1} + l_2 \mathrm{C}_{12}(\dot{q}_{d_1} + \dot{q}_{d_2}) & l_2 \mathrm{C}_{12}(\dot{q}_{d_1} + \dot{q}_{d_2}) \end{bmatrix},$$

where, for simplicity, we have used the notation $\mathrm{S}_1 = \sin(q_{d_1})$, $\mathrm{S}_2 = \sin(q_{d_2})$, $\mathrm{C}_1 = \cos(q_{d_1})$, $\mathrm{S}_{12} = \sin(q_{d_1} + q_{d_2})$, $\mathrm{C}_{12} = \cos(q_{d_1} + q_{d_2})$ .

Notice that the term $S_2$ appears in the denominator of all terms in $J(\boldsymbol{q})^{-1}$ hence, $q_{d_2} = n\pi$, with $n \in \{0, 1, 2, \ldots\}$ and any $q_{d_1}$ also correspond to singular configurations. Physically, these configurations (for any valid $n$) represent the second link being completely extended or bent over the first, as is illustrated in Figure 5.4. Typically, singular configurations are those in which the end-effector of the robot is located at the physical boundary of the workspace (that is, the physical space that the end-effector can reach). For instance, the singular configuration corresponding to being stretched out corresponds to the end-effector being placed anywhere on the circumference of radius $l_1 + l_2$, which is the boundary of the robot's workspace. As for Figure 5.4 the origin of the coordinates frame constitute another point of this boundary.

Having illustrated the inverse kinematics problem through the planar manipulator of Figure 5.2 we stop our study of inverse kinematics since it is

[1] For a definition and a detailed treatment of differential kinematics see the book (Sciavicco, Siciliano 2000) —*cf.* Bibliography at the end of Chapter 1.

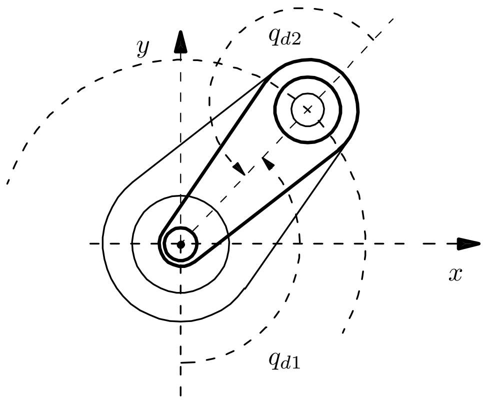


**Figure 5.4.** "Bent-over" singular configuration

beyond the scope of this text. However, we stress that what we have seen in the previous paragraphs extends in general.

In summary, we can say that if the control is based on the Cartesian coordinates of the end-effector, when designing the desired task for a manipulator's end-effector one must take special care that the configurations for the latter do not yield singular configurations. Concerning the controllers studied in this textbook, the reader should not worry about singular configurations since the Jacobian is not used at all: the reference trajectories are given in joint coordinates and we measure joint coordinates. This is what is called "control in joint space".

Thus, we leave the topic of kinematics to pass to the stage of modeling that is more relevant for control, *from the viewpoint of this* textbook, *i.e.* dynamics.

## 5.3 Dynamic Model

In this section we derive the Lagrangian equations for the CICESE prototype shown in Figure 5.1 and then we present in detail, useful bounds on the matrices of inertia, centrifugal and Coriolis forces, and on the vector of gravitational torques. Certainly, the model that we derive here applies to any planar manipulator following the same convention of coordinates as for our prototype.

### 5.3.1 Lagrangian Equations

Consider the 2-DOF robot manipulator shown in Figure 5.2. As we have learned from Chapter 3, to derive the Lagrangian dynamics we start by writing the kinetic energy function, $\mathcal{K}(\boldsymbol{q}, \dot{\boldsymbol{q}})$, defined in (3.15). For this manipulator, it may be decomposed into the sum of the two parts:

- the product of half the mass times the square of the speed of the center of mass; plus
- the product of half its moment of inertia (referred to the center of mass) times the square of its angular velocity (referred to the center of mass).

That is, we have $\mathcal{K}(\boldsymbol{q}, \dot{\boldsymbol{q}}) = \mathcal{K}_1(\boldsymbol{q}, \dot{\boldsymbol{q}}) + \mathcal{K}_2(\boldsymbol{q}, \dot{\boldsymbol{q}})$ where $\mathcal{K}_1(\boldsymbol{q}, \dot{\boldsymbol{q}})$ and $\mathcal{K}_2(\boldsymbol{q}, \dot{\boldsymbol{q}})$ are the kinetic energies associated with the masses $m_1$ and $m_2$ respectively. Let us now develop in more detail, the corresponding mathematical expressions. To that end, we first observe that the coordinates of the center of mass of link 1, expressed on the plane $x$–$y$, are

$$\begin{aligned} x_1 &= l_{c1} \sin(q_1) \\ y_1 &= -l_{c1} \cos(q_1) \,. \end{aligned}$$

The velocity vector $\boldsymbol{v}_1$ of the center of mass of such a link is then,

$$\boldsymbol{v}_1 = \begin{bmatrix} \dot{x}_1 \\ \dot{y}_1 \end{bmatrix} = \begin{bmatrix} l_{c1} \cos(q_1)\dot{q}_1 \\ l_{c1} \sin(q_1)\dot{q}_1 \end{bmatrix} .$$

Therefore, the speed squared, $\|\boldsymbol{v}_1\|^2 = \boldsymbol{v}_1^T \boldsymbol{v}_1$, of the center of mass becomes

$$\boldsymbol{v}_1^T \boldsymbol{v}_1 = l_{c1}^2 \dot{q}_1^2 \,.$$

Finally, the kinetic energy corresponding to the motion of link 1 can be obtained as

$$\begin{aligned} \mathcal{K}_1(\boldsymbol{q}, \dot{\boldsymbol{q}}) &= \frac{1}{2} m_1 \boldsymbol{v}_1^T \boldsymbol{v}_1 + \frac{1}{2} I_1 \dot{q}_1^2 \\ &= \frac{1}{2} m_1 l_{c1}^2 \dot{q}_1^2 + \frac{1}{2} I_1 \dot{q}_1^2 \,. \end{aligned} \tag{5.1}$$

On the other hand, the coordinates of the center of mass of link 2, expressed on the plane $x$–$y$ are

$$\begin{aligned} x_2 &= l_1 \sin(q_1) + l_{c2} \sin(q_1 + q_2) \\ y_2 &= -l_1 \cos(q_1) - l_{c2} \cos(q_1 + q_2) \,. \end{aligned}$$

Consequently, the velocity vector $\boldsymbol{v}_2$ of the center of mass of such a link is

$$\begin{aligned} \boldsymbol{v}_2 &= \begin{bmatrix} \dot{x}_2 \\ \dot{y}_2 \end{bmatrix} \\ &= \begin{bmatrix} l_1 \cos(q_1)\dot{q}_1 + l_{c2} \cos(q_1 + q_2)[\dot{q}_1 + \dot{q}_2] \\ l_1 \sin(q_1)\dot{q}_1 + l_{c2} \sin(q_1 + q_2)[\dot{q}_1 + \dot{q}_2] \end{bmatrix} . \end{aligned}$$

Therefore, using the trigonometric identities $\cos(\theta)^2 + \sin(\theta)^2 = 1$ and $\sin(q_1)\sin(q_1 + q_2) + \cos(q_1)\cos(q_1 + q_2) = \cos(q_2)$ we conclude that the speed squared, $\|\boldsymbol{v}_2\|^2 = \boldsymbol{v}_2^T \boldsymbol{v}_2$, of the center of mass of link 2 satisfies

$$\boldsymbol{v}_2^T \boldsymbol{v}_2 = l_1^2 \dot{q}_1^2 + l_{c2}^2 \left[\dot{q}_1^2 + 2\dot{q}_1\dot{q}_2 + \dot{q}_2^2\right] + 2 l_1 l_{c2} \left[\dot{q}_1^2 + \dot{q}_1\dot{q}_2\right] \cos(q_2)$$

which implies that

$$\begin{aligned}
\mathcal{K}_2(\boldsymbol{q}, \dot{\boldsymbol{q}}) &= \frac{1}{2} m_2 \boldsymbol{v}_2^T \boldsymbol{v}_2 + \frac{1}{2} I_2 [\dot{q}_1 + \dot{q}_2]^2 \\
&= \frac{m_2}{2} l_1^2 \dot{q}_1^2 + \frac{m_2}{2} l_{c2}^2 \left[\dot{q}_1^2 + 2\dot{q}_1\dot{q}_2 + \dot{q}_2^2\right] \\
&\quad + m_2 l_1 l_{c2} \left[\dot{q}_1^2 + \dot{q}_1\dot{q}_2\right] \cos(q_2) \\
&\quad + \frac{1}{2} I_2 [\dot{q}_1 + \dot{q}_2]^2 .
\end{aligned}$$

Similarly, the potential energy may be decomposed as the sum of the terms $\mathcal{U}(\boldsymbol{q}) = \mathcal{U}_1(\boldsymbol{q}) + \mathcal{U}_2(\boldsymbol{q})$, where $\mathcal{U}_1(\boldsymbol{q})$ and $\mathcal{U}_2(\boldsymbol{q})$ are the potential energies associated with the masses $m_1$ and $m_2$ respectively. Thus, assuming that the potential energy is zero at $y = 0$, we obtain

$$\mathcal{U}_1(\boldsymbol{q}) = -m_1 l_{c1} g \cos(q_1)$$

and

$$\mathcal{U}_2(\boldsymbol{q}) = -m_2 l_1 g \cos(q_1) - m_2 l_{c2} g \cos(q_1 + q_2) . \tag{5.2}$$

From Equations (5.1)–(5.2) we obtain the Lagrangian as

$$\begin{aligned}
\mathcal{L}(\boldsymbol{q}, \dot{\boldsymbol{q}}) &= \mathcal{K}(\boldsymbol{q}, \dot{\boldsymbol{q}}) - \mathcal{U}(\boldsymbol{q}) \\
&= \mathcal{K}_1(\boldsymbol{q}, \dot{\boldsymbol{q}}) + \mathcal{K}_2(\boldsymbol{q}, \dot{\boldsymbol{q}}) - \mathcal{U}_1(\boldsymbol{q}) - \mathcal{U}_2(\boldsymbol{q}) \\
&= \frac{1}{2}[m_1 l_{c1}^2 + m_2 l_1^2] \dot{q}_1^2 + \frac{1}{2} m_2 l_{c2}^2 \left[\dot{q}_1^2 + 2\dot{q}_1\dot{q}_2 + \dot{q}_2^2\right] \\
&\quad + m_2 l_1 l_{c2} \cos(q_2) \left[\dot{q}_1^2 + \dot{q}_1\dot{q}_2\right] \\
&\quad + [m_1 l_{c1} + m_2 l_1] g \cos(q_1) \\
&\quad + m_2 g l_{c2} \cos(q_1 + q_2) \\
&\quad + \frac{1}{2} I_1 \dot{q}_1^2 + \frac{1}{2} I_2 [\dot{q}_1 + \dot{q}_2]^2 .
\end{aligned}$$

From this last equation we obtain the following expression:

$$\begin{aligned}
\frac{\partial \mathcal{L}}{\partial \dot{q}_1} &= [m_1 l_{c1}^2 + m_2 l_1^2] \dot{q}_1 + m_2 l_{c2}^2 \dot{q}_1 + m_2 l_{c2}^2 \dot{q}_2 \\
&\quad + 2 m_2 l_1 l_{c2} \cos(q_2) \dot{q}_1 + m_2 l_1 l_{c2} \cos(q_2) \dot{q}_2 \\
&\quad + I_1 \dot{q}_1 + I_2 [\dot{q}_1 + \dot{q}_2] .
\end{aligned}$$

$$\frac{d}{dt}\left[\frac{\partial \mathcal{L}}{\partial \dot{q}_1}\right] = \left[m_1 l_{c1}^2 + m_2 l_1^2 + m_2 l_{c2}^2 + 2m_2 l_1 l_{c2}\cos(q_2)\right]\ddot{q}_1 + \left[m_2 l_{c2}^2 + m_2 l_1 l_{c2}\cos(q_2)\right]\ddot{q}_2 - 2m_2 l_1 l_{c2}\sin(q_2)\dot{q}_1\dot{q}_2 - m_2 l_1 l_{c2}\sin(q_2)\dot{q}_2^2 + I_1\ddot{q}_1 + I_2[\ddot{q}_1 + \ddot{q}_2].$$

$$\frac{\partial \mathcal{L}}{\partial q_1} = -[m_1 l_{c1} + m_2 l_1]g\sin(q_1) - m_2 g l_{c2}\sin(q_1 + q_2).$$

$$\frac{\partial \mathcal{L}}{\partial \dot{q}_2} = m_2 l_{c2}^2\dot{q}_1 + m_2 l_{c2}^2\dot{q}_2 + m_2 l_1 l_{c2}\cos(q_2)\dot{q}_1 + I_2[\dot{q}_1 + \dot{q}_2].$$

$$\frac{d}{dt}\left[\frac{\partial \mathcal{L}}{\partial \dot{q}_2}\right] = m_2 l_{c2}^2\ddot{q}_1 + m_2 l_{c2}^2\ddot{q}_2 + m_2 l_1 l_{c2}\cos(q_2)\ddot{q}_1 - m_2 l_1 l_{c2}\sin(q_2)\dot{q}_1\dot{q}_2 + I_2[\ddot{q}_1 + \ddot{q}_2].$$

$$\frac{\partial \mathcal{L}}{\partial q_2} = -m_2 l_1 l_{c2}\sin(q_2)\left[\dot{q}_1\dot{q}_2 + \dot{q}_1^2\right] - m_2 g l_{c2}\sin(q_1 + q_2).$$

The dynamic equations that model the robot arm are obtained by applying Lagrange's Equations (3.4),

$$\frac{d}{dt}\left[\frac{\partial \mathcal{L}}{\partial \dot{q}_i}\right] - \frac{\partial \mathcal{L}}{\partial q_i} = \tau_i \qquad i = 1, 2$$

from which we finally get

$$\begin{aligned}\tau_1 = {} & \left[m_1 l_{c1}^2 + m_2 l_1^2 + m_2 l_{c2}^2 + 2m_2 l_1 l_{c2}\cos(q_2) + I_1 + I_2\right]\ddot{q}_1 \\ & + \left[m_2 l_{c2}^2 + m_2 l_1 l_{c2}\cos(q_2) + I_2\right]\ddot{q}_2 \\ & - 2m_2 l_1 l_{c2}\sin(q_2)\dot{q}_1\dot{q}_2 - m_2 l_1 l_{c2}\sin(q_2)\dot{q}_2^2 \\ & + [m_1 l_{c1} + m_2 l_1]g\sin(q_1) \\ & + m_2 g l_{c2}\sin(q_1 + q_2)\end{aligned} \tag{5.3}$$

and

$$\begin{aligned}\tau_2 = {} & \left[m_2 l_{c2}^2 + m_2 l_1 l_{c2}\cos(q_2) + I_2\right]\ddot{q}_1 + [m_2 l_{c2}^2 + I_2]\ddot{q}_2 \\ & + m_2 l_1 l_{c2}\sin(q_2)\dot{q}_1^2 + m_2 g l_{c2}\sin(q_1 + q_2),\end{aligned} \tag{5.4}$$

where $\tau_1$ and $\tau_2$, are the external torques delivered by the actuators at joints 1 and 2.

Thus, the dynamic equations of the robot (5.3)-(5.4) constitute a set of two nonlinear differential equations of the state variables $\boldsymbol{x} = [\boldsymbol{q}^T\ \dot{\boldsymbol{q}}^T]^T$, that is, of the form (3.1) .

### 5.3.2 Model in Compact Form

For control purposes, it is more practical to rewrite the Lagrangian dynamic model of the robot, that is, Equations (5.3) and (5.4), in the compact form (3.18), *i.e.*

$$\underbrace{\begin{bmatrix} M_{11}(\boldsymbol{q}) & M_{12}(\boldsymbol{q}) \\ M_{21}(\boldsymbol{q}) & M_{22}(\boldsymbol{q}) \end{bmatrix}}_{M(\boldsymbol{q})} \ddot{\boldsymbol{q}} + \underbrace{\begin{bmatrix} C_{11}(\boldsymbol{q},\dot{\boldsymbol{q}}) & C_{12}(\boldsymbol{q},\dot{\boldsymbol{q}}) \\ C_{21}(\boldsymbol{q},\dot{\boldsymbol{q}}) & C_{22}(\boldsymbol{q},\dot{\boldsymbol{q}}) \end{bmatrix}}_{C(\boldsymbol{q},\dot{\boldsymbol{q}})} \dot{\boldsymbol{q}} + \underbrace{\begin{bmatrix} g_1(\boldsymbol{q}) \\ g_2(\boldsymbol{q}) \end{bmatrix}}_{\boldsymbol{g}(\boldsymbol{q})} = \boldsymbol{\tau},$$

where

$$\begin{aligned} M_{11}(\boldsymbol{q}) &= m_1 l_{c1}^2 + m_2 \left[ l_1^2 + l_{c2}^2 + 2 l_1 l_{c2} \cos(q_2) \right] + I_1 + I_2 \\ M_{12}(\boldsymbol{q}) &= m_2 \left[ l_{c2}^2 + l_1 l_{c2} \cos(q_2) \right] + I_2 \\ M_{21}(\boldsymbol{q}) &= m_2 \left[ l_{c2}^2 + l_1 l_{c2} \cos(q_2) \right] + I_2 \\ M_{22}(\boldsymbol{q}) &= m_2 l_{c2}^2 + I_2 \end{aligned}$$

$$\begin{aligned} C_{11}(\boldsymbol{q},\dot{\boldsymbol{q}}) &= -m_2 l_1 l_{c2} \sin(q_2) \dot{q}_2 \\ C_{12}(\boldsymbol{q},\dot{\boldsymbol{q}}) &= -m_2 l_1 l_{c2} \sin(q_2) \left[ \dot{q}_1 + \dot{q}_2 \right] \\ C_{21}(\boldsymbol{q},\dot{\boldsymbol{q}}) &= m_2 l_1 l_{c2} \sin(q_2) \dot{q}_1 \\ C_{22}(\boldsymbol{q},\dot{\boldsymbol{q}}) &= 0 \end{aligned}$$

$$\begin{aligned} g_1(\boldsymbol{q}) &= \left[ m_1 l_{c1} + m_2 l_1 \right] g \sin(q_1) + m_2 l_{c2} g \sin(q_1 + q_2) \\ g_2(\boldsymbol{q}) &= m_2 l_{c2} g \sin(q_1 + q_2) \,. \end{aligned}$$

We emphasize that the appropriate state variables to describe the dynamic model of the robot are the positions $q_1$ and $q_2$ and the velocities $\dot{q}_1$ and $\dot{q}_2$. In terms of these state variables, the dynamic model of the robot may be written as

$$\frac{d}{dt} \begin{bmatrix} q_1 \\ q_2 \\ \dot{q}_1 \\ \dot{q}_2 \end{bmatrix} = \begin{bmatrix} \dot{q}_1 \\ \dot{q}_2 \\ \\ M(\boldsymbol{q})^{-1} \left[ \boldsymbol{\tau}(t) - C(\boldsymbol{q},\dot{\boldsymbol{q}}) \dot{\boldsymbol{q}} - \boldsymbol{g}(\boldsymbol{q}) \right] \end{bmatrix} .$$

#### Properties of the Dynamic Model

We present now the derivation of certain bounds on the inertia matrix, the matrix of centrifugal and Coriolis forces and the vector of gravitational torques. The bounds that we derive are fundamental to properly tune the gains of the controllers studied in the succeeding chapters. We emphasize that, as studied in Chapter 4, some bounds exist for any manipulator with only revolute rigid joints. Here, we show how they can be computed for CICESE's Pelican prototype illustrated in Figure 5.2.

## Derivation of $\lambda_{\min}\{M\}$

We start with the property of positive definiteness of the inertia matrix. For a symmetric 2×2 matrix

$$\begin{bmatrix} M_{11}(\boldsymbol{q}) & M_{21}(\boldsymbol{q}) \\ M_{21}(\boldsymbol{q}) & M_{22}(\boldsymbol{q}) \end{bmatrix}$$

to be positive definite for all $\boldsymbol{q} \in \mathbb{R}^n$, it is necessary and sufficient that[2] $M_{11}(\boldsymbol{q}) > 0$ and its determinant

$$M_{11}(\boldsymbol{q})M_{22}(\boldsymbol{q}) - M_{21}(\boldsymbol{q})^2$$

also be positive for all $\boldsymbol{q} \in \mathbb{R}^n$.

In the worst-case scenario $M_{11}(\boldsymbol{q}) = m_1 l_{c1}^2 + I_1 + I_2 + m_2(l_1 - l_{c2})^2 > 0$, we only need to compute the determinant of $M(\boldsymbol{q})$, that is,

$$\begin{aligned} \det[M(\boldsymbol{q})] = I_1 I_2 &+ I_2[l_{c1}^2 m_1 + l_1^2 m_2] + l_{c2}^2 m_2 I_1 + l_{c1}^2 l_{c2}^2 m_1 m_2 \\ &+ l_1^2 l_{c2}^2 m_2^2 [1 - \cos^2(q_2)] \,. \end{aligned}$$

Notice that only the last term depends on $\boldsymbol{q}$ and is positive or zero. Hence, we conclude that $M(\boldsymbol{q})$ is positive definite for all $q \in \mathbb{R}^n$, that is[3]

$$\boldsymbol{x}^T M(\boldsymbol{q})\boldsymbol{x} \geq \lambda_{\min}\{M\}\|\boldsymbol{x}\|^2 \tag{5.5}$$

for all $\boldsymbol{q} \in \mathbb{R}^n$, where $\lambda_{\min}\{M\} > 0$.

Inequality (5.5) constitutes an important property for control purposes since for instance, it guarantees that $M(\boldsymbol{q})^{-1}$ is positive definite and bounded for all $\boldsymbol{q} \in \mathbb{R}^n$.

Let us continue with the computation of the constants $\beta$, $k_M$, $k_{C_1}$, $k_{C_2}$ and $k_g$ from the properties presented in Chapter 4.

## Derivation of $\lambda_{\mathrm{Max}}\{M\}$

Consider the inertia matrix $M(\boldsymbol{q})$. From its components it may be verified that

[2] Consider the partitioned matrix

$$\begin{bmatrix} A & B \\ B^T & C \end{bmatrix} .$$

If $A = A^T > 0$, $C = C^T > 0$ and $C - B^T A^{-1} B \geq 0$ (resp. $C - B^T A^{-1} B > 0$), then this matrix is positive semidefinite (resp. positive definite). See Horn R. A., Johnson C. R., 1985, *Matrix analysis*, p. 473.

[3] See also Remark 2.1 on page 25.

$$\max_{i,j,\boldsymbol{q}} |M_{ij}(\boldsymbol{q})| = m_1 l_{c1}^2 + m_2 \left[ l_1^2 + l_{c2}^2 + 2 l_1 l_{c2} \right] + I_1 + I_2 \,.$$

According to Table 4.1, the constant $\beta$ may be obtained as a value larger or equal to $n$ times the previous expression, *i.e.*

$$\beta \geq n \left[ m_1 l_{c1}^2 + m_2 \left[ l_1^2 + l_{c2}^2 + 2 l_1 l_{c2} \right] + I_1 + I_2 \right] \,.$$

Hence, defining, $\lambda_{\text{Max}}\{M\} = \beta$ we see that

$$\boldsymbol{x}^T M(\boldsymbol{q}) \boldsymbol{x} \leq \lambda_{\text{Max}}\{M\} \|\boldsymbol{x}\|^2$$

for all $\boldsymbol{q} \in \mathbb{R}^n$. Moreover, using the numerical values presented in Table 5.1, we get $\beta = 0.7193$ kg m$^2$, that is, $\lambda_{\text{Max}}\{M\} = 0.7193$ kg m$^2$.

### Derivation of $k_M$

Consider the inertia matrix $M(\boldsymbol{q})$. From its components it may be verified that

$$\begin{aligned}
\frac{\partial M_{11}(\boldsymbol{q})}{\partial q_1} &= 0, & \frac{\partial M_{11}(\boldsymbol{q})}{\partial q_2} &= -2 m_2 l_1 l_{c2} \sin(q_2) \\
\frac{\partial M_{12}(\boldsymbol{q})}{\partial q_1} &= 0, & \frac{\partial M_{12}(\boldsymbol{q})}{\partial q_2} &= -m_2 l_1 l_{c2} \sin(q_2) \\
\frac{\partial M_{21}(\boldsymbol{q})}{\partial q_1} &= 0, & \frac{\partial M_{21}(\boldsymbol{q})}{\partial q_2} &= -m_2 l_1 l_{c2} \sin(q_2) \\
\frac{\partial M_{22}(\boldsymbol{q})}{\partial q_1} &= 0, & \frac{\partial M_{22}(\boldsymbol{q})}{\partial q_2} &= 0 \,.
\end{aligned}$$

According to Table 4.1, the constant $k_M$ may be determined as

$$k_M \geq n^2 \left( \max_{i,j,k,\boldsymbol{q}} \left| \frac{\partial M_{ij}(\boldsymbol{q})}{\partial q_k} \right| \right) \,,$$

hence, this constant may be chosen to satisfy

$$k_M \geq n^2 2 m_2 l_1 l_{c2} \,.$$

Using the numerical values presented in Table 5.1 we get $k_M = 0.0974$ kg m$^2$.

### Derivation of $k_{C_1}$

Consider the vector of centrifugal and Coriolis forces $C(\boldsymbol{q}, \dot{\boldsymbol{q}})\dot{\boldsymbol{q}}$ written as

$$C(\boldsymbol{q}, \dot{\boldsymbol{q}})\dot{\boldsymbol{q}} = \begin{bmatrix} -m_2 l_1 l_{c2} \sin(q_2) \left( 2 \dot{q}_1 \dot{q}_2 + \dot{q}_2^2 \right) \\ \\ m_2 l_1 l_{c2} \sin(q_2) \dot{q}_1^2 \end{bmatrix}$$

$$
= \begin{bmatrix}
\begin{bmatrix} \dot{q}_1 \\ \dot{q}_2 \end{bmatrix}^T \overbrace{\begin{bmatrix} 0 & -m_2 l_1 l_{c2} \sin(q_2) \\ -m_2 l_1 l_{c2} \sin(q_2) & -m_2 l_1 l_{c2} \sin(q_2) \end{bmatrix}}^{C_1(\boldsymbol{q})} \begin{bmatrix} \dot{q}_1 \\ \dot{q}_2 \end{bmatrix} \\
\\
\begin{bmatrix} \dot{q}_1 \\ \dot{q}_2 \end{bmatrix}^T \underbrace{\begin{bmatrix} m_2 l_1 l_{c2} \sin(q_2) & 0 \\ 0 & 0 \end{bmatrix}}_{C_2(\boldsymbol{q})} \begin{bmatrix} \dot{q}_1 \\ \dot{q}_2 \end{bmatrix}
\end{bmatrix} . \tag{5.6}
$$

According to Table 4.1, the constant $k_{C_1}$ may be derived as

$$
k_{C_1} \geq n^2 \left( \max_{i,j,k,\boldsymbol{q}} \left| C_{k_{ij}}(\boldsymbol{q}) \right| \right)
$$

hence, this constant may be chosen so that

$$
k_{C_1} \geq n^2 m_2 l_1 l_{c2}
$$

Consequently, in view of the numerical values from Table 5.1 we find that $k_{C_1} = 0.0487$ kg m$^2$.

### Derivation of $k_{C_2}$

Consider again the vector of centrifugal and Coriolis forces $C(\boldsymbol{q}, \dot{\boldsymbol{q}})\dot{\boldsymbol{q}}$ written as in (5.6). From the matrices $C_1(\boldsymbol{q})$ and $C_2(\boldsymbol{q})$ it may easily be verified that

$$
\begin{aligned}
\frac{\partial C_{1_{11}}(\boldsymbol{q})}{\partial q_1} &= 0, \ \frac{\partial C_{1_{11}}(\boldsymbol{q})}{\partial q_2} = 0 \\
\frac{\partial C_{1_{12}}(\boldsymbol{q})}{\partial q_1} &= 0, \ \frac{\partial C_{1_{12}}(\boldsymbol{q})}{\partial q_2} = -m_2 l_1 l_{c2} \cos(q_2) \\
\frac{\partial C_{1_{21}}(\boldsymbol{q})}{\partial q_1} &= 0, \ \frac{\partial C_{1_{21}}(\boldsymbol{q})}{\partial q_2} = -m_2 l_1 l_{c2} \cos(q_2) \\
\frac{\partial C_{1_{22}}(\boldsymbol{q})}{\partial q_1} &= 0, \ \frac{\partial C_{1_{22}}(\boldsymbol{q})}{\partial q_2} = -m_2 l_1 l_{c2} \cos(q_2) \\
\frac{\partial C_{2_{11}}(\boldsymbol{q})}{\partial q_1} &= 0, \ \frac{\partial C_{2_{11}}(\boldsymbol{q})}{\partial q_2} = m_2 l_1 l_{c2} \cos(q_2) \\
\frac{\partial C_{2_{12}}(\boldsymbol{q})}{\partial q_1} &= 0, \ \frac{\partial C_{2_{12}}(\boldsymbol{q})}{\partial q_2} = 0 \\
\frac{\partial C_{2_{21}}(\boldsymbol{q})}{\partial q_1} &= 0, \ \frac{\partial C_{2_{21}}(\boldsymbol{q})}{\partial q_2} = 0
\end{aligned}
$$

$$\frac{\partial C_{222}(\boldsymbol{q})}{\partial q_1} = 0, \ \frac{\partial C_{222}(\boldsymbol{q})}{\partial q_2} = 0\,.$$

Furthermore, according to Table 4.1 the constant $k_{C_2}$ may be taken to satisfy

$$k_{C_2} \geq n^3 \left( \max_{i,j,k,l,\boldsymbol{q}} \left| \frac{\partial C_{k_{ij}}(\boldsymbol{q})}{\partial q_l} \right| \right)\,.$$

Therefore, we may choose $k_{C_2}$ as

$$k_{C_2} \geq n^3 m_2 l_1 l_{c2}\,,$$

which, in view of the numerical values from Table 5.1, takes the numerical value $k_{C_2} = 0.0974$ kg m$^2$:

### Derivation of $k_g$

According to the components of the gravitational torques vector $\boldsymbol{g}(\boldsymbol{q})$ we have

$$\begin{aligned}
\frac{\partial g_1(\boldsymbol{q})}{\partial q_1} &= (m_1 l_{c1} + m_2 l_1)\, g\, \cos(q_1) + m_2 l_{c2} g\, \cos(q_1 + q_2) \\
\frac{\partial g_1(\boldsymbol{q})}{\partial q_2} &= m_2 l_{c2} g\, \cos(q_1 + q_2) \\
\frac{\partial g_2(\boldsymbol{q})}{\partial q_1} &= m_2 l_{c2} g\, \cos(q_1 + q_2) \\
\frac{\partial g_2(\boldsymbol{q})}{\partial q_2} &= m_2 l_{c2} g\, \cos(q_1 + q_2)\,.
\end{aligned}$$

Notice that the Jacobian matrix $\frac{\partial \boldsymbol{g}(\boldsymbol{q})}{\partial \boldsymbol{q}}$ corresponds in fact, to the Hessian matrix (*i.e.* the second partial derivative) of the potential energy function $\mathcal{U}(\boldsymbol{q})$, and is a symmetric matrix even though not necessarily positive definite.

The positive constant $k_g$ may be derived from the information given in Table 4.1 as

$$k_g \geq n \max_{i,j,q} \left| \frac{\partial g_i(\boldsymbol{q})}{\partial q_j} \right|\,.$$

That is,

$$k_g \geq n\,[m_1 l_{c1} + m_2 l_1 + m_2 l_{c2}]\, g$$

and using the numerical values from Table 5.1 may be given the numerical value $k_g = 23.94$ kg m$^2$/s$^2$.

**Table 5.2.** Numeric values of the parameters for the CICESE prototype

| Parameter | Value | Units |
|---|---|---|
| $\lambda_{\mathrm{Max}}\{M\}$ | 0.7193 | kg m$^2$ |
| $k_M$ | 0.0974 | kg m$^2$ |
| $k_{C_1}$ | 0.0487 | kg m$^2$ |
| $k_{C_2}$ | 0.0974 | kg m$^2$ |
| $k_g$ | 23.94 | kg m$^2$/s$^2$ |

### Summary

The numerical values of the constants $\lambda_{\mathrm{Max}}\{M\}$, $k_M$, $k_{C_1}$, $k_{C_2}$ and $k_g$ obtained above are summarized in Table 5.2.

## 5.4 Desired Reference Trajectories

With the aim of testing in experiments the performance of the controllers presented in this book, on the Pelican robot, we have selected the following reference trajectories in *joint space*:

$$\begin{bmatrix} q_{d1} \\ \\ q_{d2} \end{bmatrix} = \begin{bmatrix} b_1[1 - e^{-2.0\ t^3}] + c_1[1 - e^{-2.0\ t^3}]\ \sin(\omega_1 t) \\ \\ b_2[1 - e^{-2.0\ t^3}] + c_2[1 - e^{-2.0\ t^3}]\ \sin(\omega_2 t) \end{bmatrix} \quad [\mathrm{rad}] \tag{5.7}$$

where $b_1 = \pi/4$ [rad], $c_1 = \pi/9$ [rad] and $\omega_1 = 4$ [rad/s], are parameters for the desired position reference for the first joint and $b_2 = \pi/3$ [rad], $c_2 = \pi/6$ [rad] and $\omega_2 = 3$ [rad/s] correspond to parameters that determine the desired position reference for the second joint. Figure 5.5 shows graphs of these reference trajectories against time.

Note the following important features in these reference trajectories:

- the trajectory contains a sinusoidal term to evaluate the performance of the controller following relatively fast periodic motions. This test is significant since such motions excite nonlinearities in the system.
- It also contains a slowly increasing term to bring the robot to the operating point without driving the actuators into saturation.

The module and frequency of the periodic signal must be chosen with care to avoid both torque and speed saturation in the actuators. In other

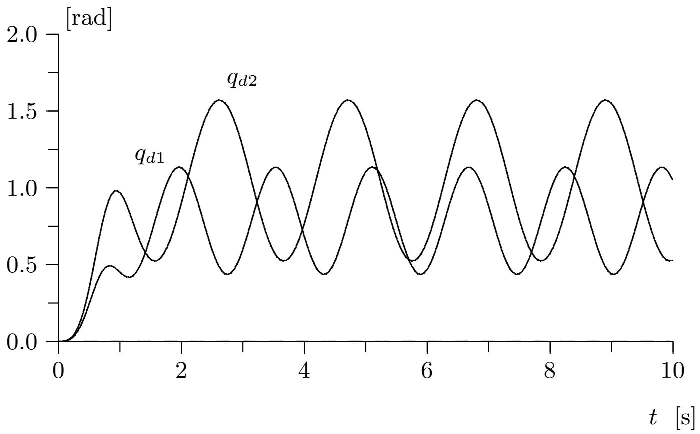


**Figure 5.5.** Desired reference trajectories

words, the reference trajectories must be such that the evolution of the robot dynamics along these trajectories gives admissible velocities and torques for the actuators. Otherwise, the desired reference is physically unfeasible.

Using the expressions of the desired position trajectories, (5.7), we may obtain analytically expressions for the desired velocity reference trajectories. These are obtained by direct differentiation, *i.e.*

$$\dot{q}_{d1} = 6b_1t^2e^{-2.0\ t^3} + 6c_1t^2e^{-2.0\ t^3}\sin(\omega_1t) + [c_1 - c_1e^{-2.0\ t^3}]\cos(\omega_1t)\omega_1,$$
$$\dot{q}_{d2} = 6b_2t^2e^{-2.0\ t^3} + 6c_2t^2e^{-2.0\ t^3}\sin(\omega_2t) + [c_2 - c_2e^{-2.0\ t^3}]\cos(\omega_2t)\omega_2\,, \tag{5.8}$$

in [ rad/s ]. In the same way we may proceed to compute the reference accelerations to obtain

$$\begin{aligned}\ddot{q}_{d1} &= 12b_1te^{-2.0\ t^3} - 36b_1t^4e^{-2.0\ t^3} + 12c_1te^{-2.0\ t^3}\sin(\omega_1t)\\ &\quad - 36c_1t^4e^{-2.0\ t^3}\sin(\omega_1t) + 12c_1t^2e^{-2.0\ t^3}\cos(\omega_1t)\omega_1\\ &\quad - [c_1 - c_1e^{-2.0\ t^3}]\sin(\omega_1t)\omega_1^2 \qquad [\mathrm{rad/s^2}]\,,\end{aligned}$$

$$\begin{aligned}\ddot{q}_{d2} &= 12b_2te^{-2.0\ t^3} - 36b_2t^4e^{-2.0\ t^3} + 12c_2te^{-2.0\ t^3}\sin(\omega_2t)\\ &\quad - 36c_2t^4e^{-2.0\ t^3}\sin(\omega_2t) + 12c_2t^2e^{-2.0\ t^3}\cos(\omega_2t)\omega_2\\ &\quad - [c_2 - c_2e^{-2.0\ t^3}]\sin(\omega_2t)\omega_2^2 \qquad [\mathrm{rad/s^2}]\,.\end{aligned} \tag{5.9}$$

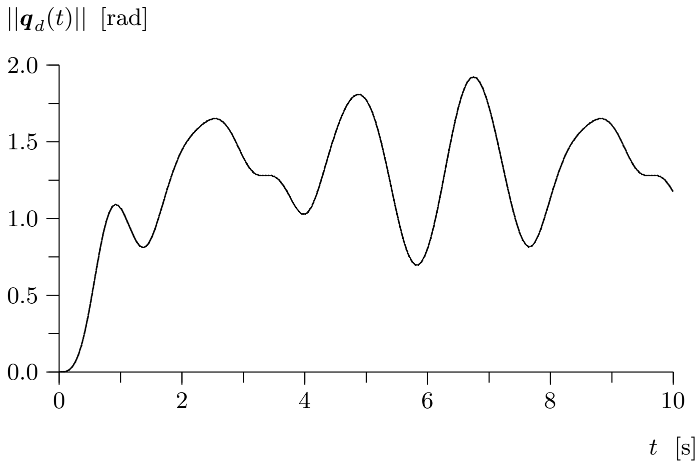


**Figure 5.6.** Norm of the desired positions

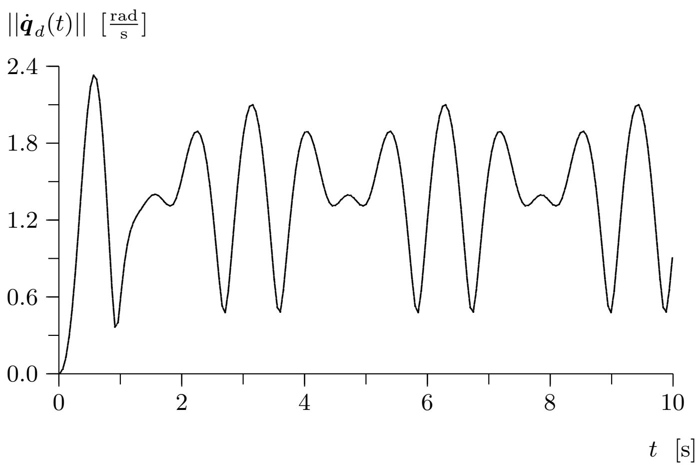


**Figure 5.7.** Norm of the desired velocities vector

Figures 5.6, 5.7 and 5.8 show the evolution in time of the norms corresponding to the desired joint positions, velocities and accelerations respectively. From these figures we deduce the following upper-bounds on the norms

$$
\begin{aligned}
\|\boldsymbol{q}_d\|_{\mathrm{Max}} &\leq 1.92 \text{ [rad]} \\
\|\dot{\boldsymbol{q}}_d\|_{\mathrm{Max}} &\leq 2.33 \text{ [rad/s]} \\
\|\ddot{\boldsymbol{q}}_d\|_{\mathrm{Max}} &\leq 9.52 \text{ [rad/s}^2] \,.
\end{aligned}
$$

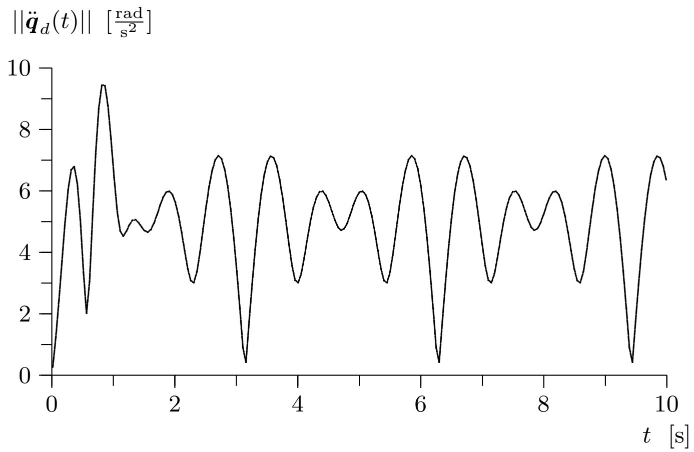


**Figure 5.8.** Norm of the desired accelerations vector

## Bibliography

The schematic diagram of the robot depicted in Figure 5.2 and elsewhere throughout the book, corresponds to a real experimental prototype robot arm designed and constructed in the CICESE Research Center, Mexico[4].

The numerical values that appear in Table 5.1 are taken from:

- Campa R., Kelly R., Santibáñez V., 2004, *"Windows-based real-time control of direct-drive mechanisms: platform description and experiments"*, Mechatronics, Vol. 14, No. 9, pp. 1021–1036.

The constants listed in Table 5.2 may be computed based on data reported in

- Moreno J., Kelly R., Campa R., 2003, *"Manipulator velocity control using friction compensation"*, IEE Proceedings - Control Theory and Applications, Vol. 150, No. 2.

## Problems

1. Consider the matrices $M(\boldsymbol{q})$ and $C(\boldsymbol{q}, \dot{\boldsymbol{q}})$ from Section 5.3.2. Show that the matrix $\left[\frac{1}{2}\dot{M}(\boldsymbol{q}) - C(\boldsymbol{q}, \dot{\boldsymbol{q}})\right]$ is skew-symmetric.
2. According to Property 4.2, the centrifugal and Coriolis forces matrix $C(\boldsymbol{q}, \dot{\boldsymbol{q}})$, of the dynamic model of an $n$-DOF robot is not unique. In Section 5.3.2 we computed the elements of the matrix $C(\boldsymbol{q}, \dot{\boldsymbol{q}})$ of the Pelican

[4] "Centro de Investigación Científica y de Educación Superior de Ensenada".

robot presented in this chapter. Prove also that the matrix $C(\boldsymbol{q}, \dot{\boldsymbol{q}})$ whose elements are given by

$$
\begin{aligned}
C_{11}(\boldsymbol{q}, \dot{\boldsymbol{q}}) &= -2m_2 l_1 l_{c2} \sin(q_2)\dot{q}_2 \\
C_{12}(\boldsymbol{q}, \dot{\boldsymbol{q}}) &= -m_2 l_1 l_{c2} \sin(q_2)\dot{q}_2 \\
C_{21}(\boldsymbol{q}, \dot{\boldsymbol{q}}) &= m_2 l_1 l_{c2} \sin(q_2)\dot{q}_1 \\
C_{22}(\boldsymbol{q}, \dot{\boldsymbol{q}}) &= 0
\end{aligned}
$$

characterizes the centrifugal and Coriolis forces, $C(\boldsymbol{q}, \dot{\boldsymbol{q}})\dot{\boldsymbol{q}}$. With this definition of $C(\boldsymbol{q}, \dot{\boldsymbol{q}})$, is $\frac{1}{2}\dot{M}(\boldsymbol{q}) - C(\boldsymbol{q}, \dot{\boldsymbol{q}})$ skew-symmetric?

Does it hold that $\dot{\boldsymbol{q}}^T \left[\frac{1}{2}\dot{M}(\boldsymbol{q}) - C(\boldsymbol{q}, \dot{\boldsymbol{q}})\right] \dot{\boldsymbol{q}} = 0$ ? Explain.